Phase Reassignment with Efficient Estimation of Phase Difference

Maria Åkesson
Centre for Mathematical Sciences
Lund University
Lund, Sweden
Email: maria.akesson@matstat.lu.se

Maria Sandsten
Centre for Mathematical Sciences
Lund University
Lund, Sweden
Email: maria.sandsten@matstat.lu.se

***Abstract*—The recently developed Matched Phase Reassignment (MPR) gives a time-frequency local measure of phase difference between short oscillatory transient signals. However, the resulting phase estimate is not satisfactory as it has poor resolution for high oscillatory frequencies. The MPR is also sensitive to high noise levels and is computationally cumbersome.**

In this paper, a novel reassignment method for phase difference estimation is proposed and evaluated. In comparison to the MPR the accuracy is increased and the computational time is reduced. Simulations show that the proposed technique also outperforms state-of-the-art methods in terms of efficiency. An illustrative example of phase difference estimates of the electrical signals measured from the brain is included.

I. Introduction

Time-frequency (TF) methods are used in many application areas, such as vibration analysis, radar detection, geophysics, and medicine. The measured signals are often time-varying and of oscillatory character. State-of-the-art methods aim at increased concentration of components and suppression of cross-terms using the quadratic class of TF representations [1]. More modern ridge detection methods aim to track the frequency changes in the TF images. The TF reassignment and synchrosqueezing techniques, [2]–[4], are well known techniques for sharpening the ridges in a TF image, and have in recent years been further developed e.g. in [5]–[7]. We have recently invented a matched reassigned spectrogram (MRS) method, tailored to give perfect instantaneous time and frequency mass localization for short oscillating transients, [8]–[11].

We have also expanded the MRS into a matched phase reassignment (MPR) method based on the reassigned cross-spectrogram, [12]. For two phase synchronized oscillating transient signals, the method gives perfect instantaneous time and frequency mass localization. The MPR is thereby a TF local measure of phase synchronization and can also be used to measure the actual phase difference between short transient signals by time-shifting one signal until perfect localization is achieved. However, in its present form, the resulting phase estimate is not satisfactory as it is limited by the sampling frequency. Moreover, the MPR for phase-estimation is computationally cumbersome, especially for low frequency signals.

Electroencephalography (EEG) is well suited for estimation of the temporal dynamics of neural activity [13], and with multi-dimensional measurements, the synchronization of sources can be estimated on a ms time-scale. Oscillating transients are an appropriate model of such event-related responses in cognition experiments [14].

In this submission we further explore a novel technique to measure the phase difference, and compare to commonly used phase estimators, for different types of disturbances. We start with a short presentation of the MRS and MPR techniques in section 2 followed by a description of the proposed phase estimator in section 3. In section 4, the performance of the proposed technique compared to state-of-the-art estimators is evaluated, especially for estimation of phase difference. An example of phase estimates from transient responses in the measured electrical activity from the brain is also given. Conclusions are presented in section 5.

II. The Matched Reassignment Technique

The reassigned spectrogram of a signal x is defined as

$$RS_x^h(t,\omega) = \iint S_x^h(s,\xi)\delta(t-\hat{t}(s,\xi),\omega-\hat{\omega}(s,\xi))\mathrm{d}s\frac{\mathrm{d}\xi}{2\pi}, \quad (1)$$

where the integrals run from $-\infty$ to ∞ and $\delta(t,\omega)$ denotes the Dirac-delta function. The spectrogram S_x^h is given by

$$S_x^h(t,\omega) = F_x^h(t,\omega)(F_x^h(t,\omega))^* \quad (2)$$

where * denotes the complex conjugate. The Fourier transform (FT) of x using window function h is defined as

$$F_x^h(t,\omega) = \int x(\tau)h^*(\tau-t)e^{-i\omega\tau}\mathrm{d}\tau. \quad (3)$$

The reassignment vectors are further given by

$$\hat{t}(t,\omega) = t + c_t\Re\left(\frac{F_x^{th}(t,\omega)}{F_x^h(t,\omega)}\right) \quad (4)$$

$$\hat{\omega}(t,\omega) = \omega - c_\omega\Im\left(\frac{F_x^{\mathrm{d}h/\mathrm{d}t}(t,\omega)}{F_x^h(t,\omega)}\right), \quad (5)$$

where $\Re$ and $\Im$ denotes the real and imaginary part respectively. The reassignment vectors relocate the energy in (t,ω) to a new point $(\hat{t}(t,\omega),\hat{\omega}(t,\omega))$. Choosing $c_t = c_\omega = 1$ gives the reassignment vectors known from [2], [3]. If the signal is additionally assumed to be a oscillating transient of the form

$$x(t) = a(t-t_0)e^{-i\omega_0 t}. \quad (6)$$

Furthermore assuming that the spectrogram uses a window matching the signal envelope, such that $h(t) = a(-t)$, the Matched Reassigned Spectrogram (MRS) will perfectly localize the signal energy to (t_0, ω_0) choosing $c_t = c_\omega = 2$ [8], [9].

In [12], the MRS was further extended to a Matched Phase Reassignment (MPR) technique based on cross-spectrograms. For the MPR, we assume two oscillating transients with different phases and amplitudes, such that

$$y_n(t) = A_n x(t) \mathrm{e}^{-i\phi_n}, \quad n = 1, 2. \tag{7}$$

The reassigned cross-spectrogram of y_1 and y_2 can be constructed as in (1), but the spectrogram is exchanged for the absolute value of the cross-spectrogram

$$|S^h_{y_1,y_2}(t,\omega)| = |F^h_{y_1}(t,\omega)(F^h_{y_2}(t,\omega))^*|. \tag{8}$$

The reassignment vectors are given by

$$\hat{t}(t,\omega) = t + c_t \Re\left(\frac{F^{th}_{y_1}(t,\omega)}{F^h_{y_2}(t,\omega)} + \frac{F^{th}_{y_2}(t,\omega)}{F^h_{y_1}(t,\omega)}\right) \tag{9}$$

$$\hat{\omega}(t,\omega) = \omega - c_\omega \Im\left(\frac{F^{\frac{\mathrm{d}h}{\mathrm{d}t}}_{y_1}(t,\omega)}{F^h_{y_2}(t,\omega)} + \frac{F^{\frac{\mathrm{d}h}{\mathrm{d}t}}_{y_2}(t,\omega)}{F^h_{y_1}(t,\omega)}\right), \tag{10}$$

where we find that

$$F^h_{y_n}(t,\omega) = A_n e^{-i\phi_n} F^h_x(t,\omega) \tag{11}$$

$$F^{th}_{y_n}(t,\omega) = A_n e^{-i\phi_n} F^{th}_x(t,\omega) \tag{12}$$

$$F^{\frac{dh}{dt}}_{y_n}(t,\omega) = A_n e^{-i\phi_n} F^{\frac{dh}{dt}}_x(t,\omega). \tag{13}$$

As a consequence of this, the MPR vectors will coincide with the MRS vectors in (4) (5) if $\Delta\phi = \phi_1 - \phi_2 = 0$ and $c_t = c_\omega = 2\frac{A_1A_2}{A_1^2+A_2^2}$, giving perfect localization in the TF-domain.

A. Relative phase estimation using MPR

In [12], the MPR was used for estimating the relative phase-difference between two oscillating transients. As the relative phase difference $\Delta\phi$ corresponds to a time-shift k, it can be reasonably estimated by the candidate time-shift k_c which gives the most localized energy in TF. This corresponds to finding the time-shift which minimizes the Rényi entropy

$$RE = \frac{1}{1-\alpha}\log_2 \iint_A \left(\frac{RS(t,\omega)}{\iint_A RS(s,\xi)\mathrm{d}s\,\mathrm{d}\xi}\right)^\alpha \mathrm{d}t\,\mathrm{d}\omega \tag{14}$$

where $\alpha = 3$ and A is a chosen area in TF [15]. However, the technique is limited by the chosen sampling frequency, thus fewer k_c will correspond to phase differences between $-\pi$ and π for higher frequencies.

III. The Phase-Scaled Reassignment

In order to increase resolution of the relative phase estimations, we propose a novel Phase-Scaled Reassignment (PSR) approach using the following reassignment vectors

$$\hat{t}(t,\omega) = t + c_0 \Re\left(c_{t_1}\frac{F^{th}_{y_1}(t,\omega)}{F^h_{y_2}(t,\omega)} + c_{t_2}\frac{F^{th}_{y_2}(t,\omega)}{F^h_{y_1}(t,\omega)}\right) \tag{15}$$

$$\hat{\omega}(t,\omega) = \omega - c_0 \Im\left(c_{\omega_1}\frac{F^{\frac{\mathrm{d}h}{\mathrm{d}t}}_{y_1}(t,\omega)}{F^h_{y_2}(t,\omega)} + c_{\omega_2}\frac{F^{\frac{\mathrm{d}h}{\mathrm{d}t}}_{y_2}(t,\omega)}{F^h_{y_1}(t,\omega)}\right), \tag{16}$$

where c_{t_1}, c_{t_2}, c_{ω_1} and c_{ω_2} are tunable using candidate relative phase differences $\Delta\phi_c$. Using the relations in (11)-(13), the reassignment vectors can be simplified to

$$\hat{t}(t,\omega) = t + c_0 \Re\left((c_{t_1}\frac{A_1}{A_2}e^{-i\Delta\phi} + c_{t_2}\frac{A_2}{A_1}e^{i\Delta\phi})\frac{F^{th}_x}{F^h_x}\right) \tag{17}$$

$$\hat{\omega}(t,\omega) = \omega - c_0 \Im\left((c_{\omega_1}\frac{A_1}{A_2}e^{-i\Delta\phi} + c_{\omega_2}\frac{A_2}{A_1}e^{i\Delta\phi})\frac{F^{\frac{dh}{dt}}_x}{F^h_x}\right), \tag{18}$$

where the indexing of $F^h_x(t,\omega)$, $F^{th}_x(t,\omega)$, $F^{\frac{dh}{dt}}_x(t,\omega)$ has been dropped for convenience.

Perfect localization can be achieved for two sets of constants. In the first set, only one term in (15) and (16) is included and the constants are either defined as

$$c_0 = 2 \tag{19}$$

$$c_{t_1} = c_{\omega_1} = \frac{\hat{A}_2}{\hat{A}_1}e^{i\Delta\phi_c} \tag{20}$$

$$c_{t_2} = c_{\omega_2} = 0, \tag{21}$$

or as $c_{t_1} = c_{\omega_1} = 0$, $c_{t_2} = c_{\omega_2} = \hat{A}_1/\hat{A}_2 e^{-i\Delta\phi_c}$, where $\hat{A}_n$ is the estimated amplitude of signal n and $\Delta\phi_c$ is a candidate phase difference. If $\Delta\phi_c = \Delta\phi$, $\hat{A}_1 = A_1$ and $\hat{A}_2 = A_2$, (17), (18) reduces to (4), (5) and perfect localization is achieved. From hereon the reassignment made with this set of constants will be referred to as PSR1.

The other set of constants include both terms, such that

$$c_0 = 1 \tag{22}$$

$$c_{t_1} = c_{\omega_1} = \frac{\hat{A}_2}{\hat{A}_1}e^{i\Delta\phi_c} \tag{23}$$

$$c_{t_2} = c_{\omega_2} = \frac{\hat{A}_1}{\hat{A}_2}e^{-i\Delta\phi_c}, \tag{24}$$

which we will refer to as PSR2. In the same way as before, perfect localization is achieved when $\Delta\phi_c = \Delta\phi$, $\hat{A}_1 = A_1$ and $\hat{A}_2 = A_2$.

A. Relative phase estimation using PSR

The PSR can be used to estimate the phase difference between two oscillating transients. For the PSR, the estimated phase difference $\Delta\hat{\phi}$ is given by the candidate phase difference $\Delta\phi_c$ which minimizes the Rényi entropy of the reassigned cross-spectrogram. This is exemplified in Fig. 1, where the Rényi entropy is plotted for different candidates $\Delta\phi_c$. It is clearly seen that the PSR cross-spectrogram becomes more peaked the closer $\Delta\phi_c$ is to the true $\Delta\phi$. In contrast to the MPR estimations, this technique is not limited by the chosen sampling frequency as $\Delta\phi_c$ can be arbitrarily chosen. Moreover, as the resulting phase estimates using either set of constants are correlated, no precision can be gained by averaging the estimates.

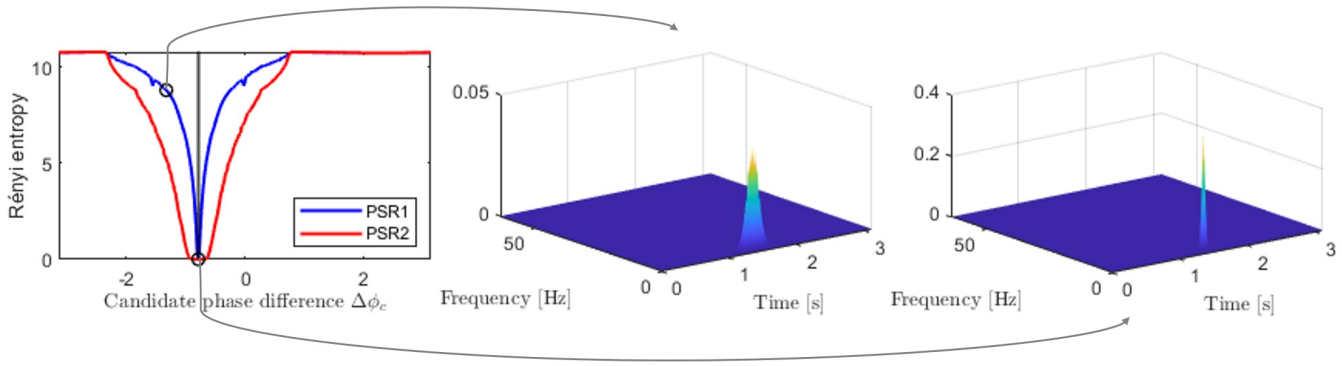

Fig. 1. The Rényi entropy evaluated over reassigned cross-spectrograms, using different candidate phase differences $\Delta\phi_c$ in the reassignment vectors. The gray line represents the true phase difference between the signals, which is $\Delta\phi = -\pi/5$. The corresponding cross-spectrograms for two different $\Delta\phi_c$ are illustrated to the right.

B. The problem with using two terms

How will the number of terms used in (15) and (16) affect the resulting phase-estimates? As the quadratic class of distributions obey TF invariance, the analysis will be restricted to $(t_0, \omega_0) = (0, 0)$. In [9], the following expressions were derived

$$F_x^h(t,\omega) = e^{-i\frac{\omega t}{2}} R_1(t,\omega) \tag{25}$$

$$F_x^{th}(t,\omega) = e^{-i\frac{\omega t}{2}} \left(I_1(t,\omega) - \frac{t}{2} R_1(t,\omega) \right) \tag{26}$$

$$F_x^{\frac{dh}{dt}}(t,\omega) = e^{-i\frac{\omega t}{2}} \left(i\frac{\omega}{2} R_1(t,\omega) - i I_2(t,\omega) \right), \tag{27}$$

where R_1 is a real valued expression and I_1 and I_2 are purely imaginary. From hereon, the indexing of F_x^h, F_x^{th}, $F_x^{\frac{dh}{dt}}$, R_1, I_1 and I_2 will be dropped for convenience.

Let's first consider PSR1, and let's further assume that $\Delta\phi_c = \Delta\phi + \epsilon$, where ϵ is a small deviance from the sought phase difference. In order to simplify the calculations we also assume that the amplitudes are known and equal to one. Then, the reassignment vectors in (17) and (18) can be simplified to

$$\begin{aligned}
\hat{t}(t,\omega) &= t + 2\Re\left(e^{i\epsilon} \frac{F_x^{th}}{F_x^h} \right) = \\
&= t + 2\Re\left((\cos(\epsilon) + i\sin(\epsilon)) \frac{e^{-i\frac{\omega t}{2}} (I_1 - \frac{t}{2} R_1)}{e^{-i\frac{\omega t}{2}} R_1} \right) = \\
&= t + 2\sin(\epsilon)\frac{iI_1}{R_1} - \cos(\epsilon)t \approx 2\epsilon\frac{iI_1}{R_1}
\end{aligned} \tag{28}$$

and

$$\begin{aligned}
\hat{\omega}(t,\omega) &= \omega - 2\Im\left(e^{i\epsilon} \frac{F_x^{\frac{dh}{dt}}}{F_x^h} \right) = \\
&= \omega - 2\Im\left((\cos(\epsilon) + i\sin(\epsilon)) \frac{e^{-i\frac{\omega t}{2}} (i\frac{\omega}{2} R_1 - i I_2)}{e^{-i\frac{\omega t}{2}} R_1} \right) = \\
&= \omega + 2\sin(\epsilon)\frac{iI_2}{R_1} - \cos(\epsilon)\omega \approx 2\epsilon\frac{iI_2}{R_1}
\end{aligned} \tag{29}$$

assuming that ϵ is sufficiently close to zero. Perfect localization is achieved only when ϵ exactly equals zero.

When instead PSR2 is considered, (17) and (18) are simplified to

$$\begin{aligned}
\hat{t}(t,\omega) &= t + \Re\left((e^{i\epsilon} + e^{-i\epsilon}) \frac{F_x^{th}}{F_x^h} \right) = \\
&= t + \Re\left(2\cos(\epsilon) \frac{e^{-i\frac{\omega t}{2}} (I_1 - \frac{t}{2} R_1)}{e^{-i\frac{\omega t}{2}} R_1} \right) = \\
&= t - \cos(\epsilon)t \approx 0,
\end{aligned} \tag{30}$$

and

$$\begin{aligned}
\hat{\omega}(t,\omega) &= \omega - \Im\left((e^{i\epsilon} + e^{-i\epsilon}) \frac{F_x^{\frac{dh}{dt}}}{F_x^h} \right) = \\
&= \omega - \Im\left(2\cos(\epsilon) \frac{e^{-i\frac{\omega t}{2}} (i\frac{\omega}{2} R_1 - i I_2)}{e^{-i\frac{\omega t}{2}} R_1} \right) = \\
&= \omega - \cos(\epsilon)\omega \approx 0,
\end{aligned} \tag{31}$$

when ϵ is sufficiently small. The PSR2 will therefor be perfectly localized in TF for several $\Delta\phi_c$ close to $\Delta\phi$.

This causes the relative phase-estimates of PSR2 to become less precise than those of PSR1. This is illustrated in Fig. 2 (a), where two 4 Hz oscillating Gaussian transients with a relative phase of $\Delta\phi = -\pi/5$ are plotted. The signals are further disturbed by additive Gaussian noise sequences where the noise sequences are white and uncorrelated. The Rényi entropy of the corresponding PSR cross-spectrograms for different candidate phases $\Delta\phi_c$ are plotted in Fig. 2 (b). It is clearly seen that PSR2 will have difficulty finding a precise estimate of the relative phase.

IV. Simulations

In all simulations, the real-part of the signals defined in (7) are considered, where $A_1 = 1$, $t_0 = 1.5$ s, $f_0 = 4$ Hz and $\phi_1 \in \mathcal{U}(-\pi, \pi)$. The amplitude of the second signal was $A_2 = 1$, and the phase was given by $\phi_2 = \phi_1 - \Delta\phi$, where the relative phase $\Delta\phi$ was randomly selected from 32 different, equally spaced candidates in $[-\pi, \pi[$. The signal envelopes are given by Gaussian windows with scaling parameter $\sigma = 20$. The signals are $N = 400$ samples long and are sampled with

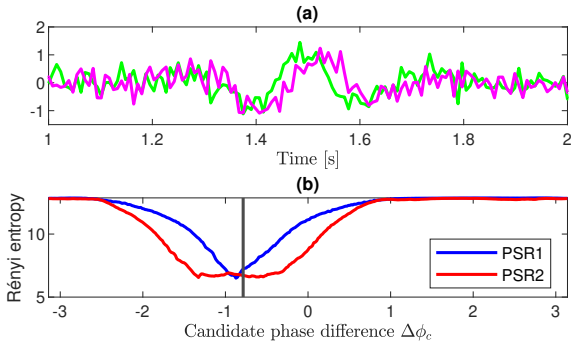

Fig. 2. In (a) the SNR=-3 is exemplified for two oscillating Gaussian transients with $f_0 = 4$ Hz, t_0=1.5 s, $\sigma = 20$ and $\Delta\phi = -\pi/5$. In (b) the Rényi entropies of the corresponding reassigned cross-spectrograms using either PSR1 or PSR2 are plotted for different choices of $\Delta\phi_c$.

TABLE I
AVERAGE COMPUTATION TIME OVER 1000 SIMULATIONS EVALUATING 32 DIFFERENT CANDIDATES.

PSR1	PSR2	MPR
0.2598 s	0.3241 s	1.1698 s

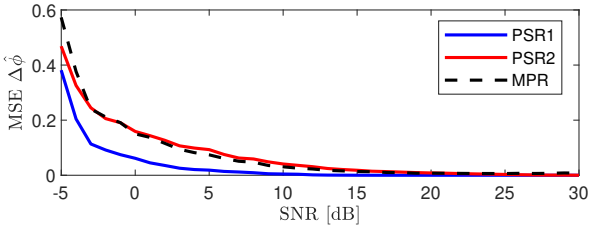

Fig. 3. The resulting MSE of the two proposed PSR methods as well as the previously proposed MPR method for estimation of phase-difference.

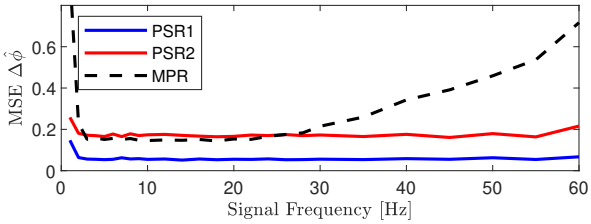

Fig. 4. The MSE of the resulting phase estimates for different signal frequencies at SNR = 0.

a sampling frequency of $F_s = 128$ Hz. White Gaussian noise is further added to the signals, where the signal-to-noise ratio (SNR) is defined as the average signal energy within $t_0 \pm 3\sigma$ over the noise variance. In Fig. 2 (a), the signals for SNR$=-3$ dB are exemplified. All simulations were performed on MATLAB (R2020a) on a computer with a 11 Generation Intel Core i7 (11700K) processor running at 3.60 GHz.

A. Comparison to the MPR

We start by comparing the relative phase estimations of the PSR method to the previously proposed MPR method. The two PSR methods were evaluated for the same 32 candidates, $\Delta\phi_c$, and the MPR was evaluated for the corresponding time lags, $k_c = -16, ..., 15$. One thousand simulations were made for each SNR level.

The mean square error (MSE) of the resulting phase estimates are plotted in Fig. 3. As expected, the PSR1 results in lower MSE than the other two methods that use two terms in the reassignment. The corresponding average computation times are presented in Table I. As the MPR in contrast to PSR computes new FTs for each k_c, it is far more computationally cumbersome than the PSR methods. Moreover, as the PSR1 needs fewer FTs than the PSR2, it is slightly faster. However, it is worth noting that the computation time will scale with the number of $\Delta\phi_c$. In the following simulations, the number of evaluated $\Delta\phi_c$ will be increased in order to improve the estimation accuracy.

The methods were further compared for different signal frequencies at SNR=0. Now, the relative phase-differences were randomly simulated from $\mathcal{U}(-\pi, \pi)$, and the PSR methods were evaluated for 180 equally spaced candidates in $[-\pi, \pi[$. As the MPR is limited by the sampling frequency, it was evaluated for the maximum number of possible time-lags covering phase-differences between $-\pi$ and π for each frequency.

The simulation results are shown in Fig 4. We note that the PSR estimates are consistent for all signal frequencies, whereas the MSE using the MPR grows with increased frequency. As fewer time-lags k_c can be evaluated for higher frequencies, the MSE naturally increases.

B. Comparison to state-of-the-art methods

The PSR1 method was also compared to the state-of-the-art phase estimators Pearson's linear correlation (CORR) and the Hilbert transform. CORR was evaluated like the MPR for 32 different time-lags. The Hilbert transform was used to estimate the instantaneous phase-difference $\Delta\hat{\phi}(t_k) = \hat{\phi}_1(t_k) - \hat{\phi}_2(t_k)$ for all K samples between 1 and 2 s, and was finally averaged according to

$$\Delta\hat{\phi}_H = \arg\left(\frac{1}{K}\sum_{k=1}^{K} e^{i\Delta\hat{\phi}(t_k)}\right). \tag{32}$$

In this simulation, the second signal was further assumed to be of varying amplitude such that $A_2 = A_1 + \delta$, where $\delta \in \mathcal{U}(-0.5, 0.5)$. In the PSR1, the amplitude of each signal was estimated as the square root of the maximum value in the spectrogram.

The simulation results are presented in Fig. 5 where it becomes clear that the PSR1 outperforms the two state-of-the-art estimators in both high and low SNR. In (a), the percentage correctly estimated phase differences for each method is plotted against SNR. The estimate was considered correct if it was less than 2.5° from the true value. As the CORR estimator is limited by the sampling frequency in the same way as the MPR method was, it is unsurprising that the accuracy of this method is poor. In contrast, even though the Hilbert estimator

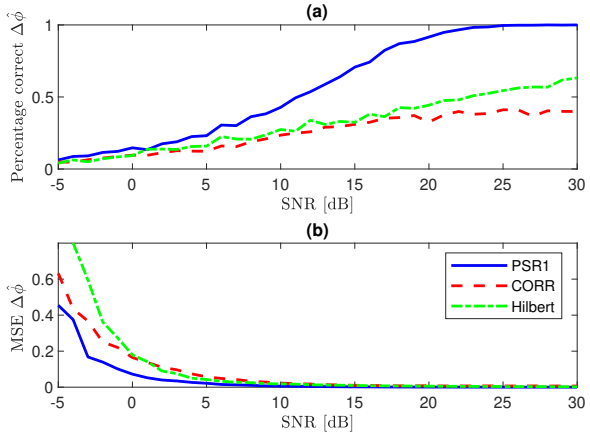

Fig. 5. In (a), the percentage correctly estimated relative phases for different SNR levels. The corresponding MSE of the estimates are plotted in (b).

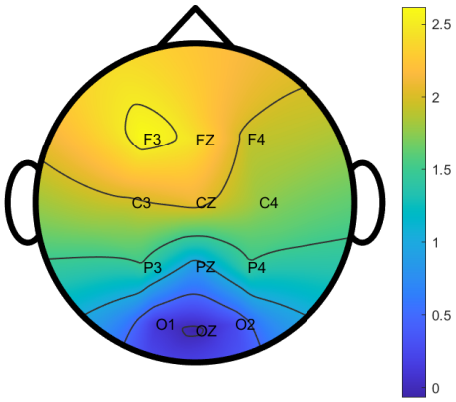

Fig. 6. The figure shows the estimated relative phases between all channels and Oz placed at the back of the head.

is not limited by a grid of candidates, it is still outperformed by the PSR1 even in high SNR. From (b) we draw the conclusion that the PSR1 estimator is considerably more efficient than the other estimators even in low SNR.

C. Phase difference estimation in EEG

Finally, we aim to estimate the relative phase-difference between channels in a EEG data set. The data was measured during visual stimulation. The subject had their eyes closed and was presented with 9 Hz flickering light (Grass Photic stimulator Model PS22C) for a duration of 1.0 s. The data was recorded with a sampling frequency of 256 Hz using a Neuroscan system with a digital amplifier (SYNAP 5080, Neuro Scan, Inc.). Amplifier band-pass settings were 0.3 and 50 Hz. The phase differences for all channels relative to the occipital channel Oz were estimated using the PSR1 method. A Gaussian window with an approximate length of one second was used in the Fourier transforms and 180 equally spaced candidate phase differences in $[-\pi, \pi[$ were evaluated. Evaluation was limited to frequencies between 8 and 10 Hz.

The resulting estimates are illustrated in Fig. 6. The results are expected, where the largest phase differences are found for channels close to the eyes. The phase difference between Oz and Fz was estimated to 2.44, which corresponds to a time difference of 43 ms for a 9 Hz signal.

V. Conclusion

The Phase-Scaled Reassignment (PSR) is proposed to estimate phase-difference between two oscillating transient signals. In contrast to the previously proposed Matched Phase Reassignment (MPR) method, it was analytically shown that more efficient estimates could be made when only one term was included in the reassignment vectors. This method was further shown to outperform the state-of-the-art methods in terms of efficiency in both high and low SNRs for white Gaussian noise disturbance.

References

[1] L. Cohen, *Time-Frequency Analysis*, ser. Signal Processing Series. Upper Saddle River, NJ, USA: Prentice-Hall, 1995.

[2] K. Kodera, C. de Villedary, and R. Gendrin, "A new method for the numerical analysis of nonstationary signals," *Physics of the Earth & Planetary Interiors*, vol. 12, pp. 142–150, 1976.

[3] F. Auger and P. Flandrin, "Improving the readability of time-frequency and time-scale representations by the reassignment method," *IEEE Trans. on Signal Processing*, vol. 43, pp. 1068–1089, May 1995.

[4] I. Daubechies, Y. G. Wang, and H.-T. Wu, "ConceFT: concentration of frequency and time via a multitapered synchrosqueezed transform." *Phil. Trans. R. Soc. A*, vol. 374, no. 20150193, 2016.

[5] K. Abratkiewicz and P. Samczynski, "Multitaper time-frequency reassigned spectrogram in micro-doppler radar signal analysis." *Signal Processing Symposium (SPSympo), 2021*, pp. 1 – 5, 2021.

[6] S. Meignen and P. Duong-Hung, "Retrieval of the modes of multicomponent signals from downsampled short-time Fourier transform." *IEEE Trans. on Signal Processing*, vol. 66, no. 23, pp. 6204 – 6215, 2018.

[7] D. Fourer, F. Auger, and G. Peeters, "Local AM/FM parameters estimation: Application to sinusoidal modeling and blind audio source separation," *IEEE Signal Processing Letters*, vol. 25, no. 10, pp. 1600–1604, 2018.

[8] J. Brynolfsson, I. Reinhold, and M. Sandsten, "A time-frequency-shift invariant parameter estimator for oscillating transient functions using the matched window reassignment," *Signal Processing*, vol. 183, 2021, 107913.

[9] M. Sandsten, J. Brynolfsson, and I. Reinhold, "The matched window reassignment," in *Proceedings of the EUSIPCO*, Rome, Italy, 2018.

[10] J. Brynolfsson and M. Sandsten, "Parameter estimation of oscillating Gaussian functions using the scaled reassigned spectrogram," *Signal Processing*, vol. 150, pp. 20–32, 2018.

[11] M. Hansson-Sandsten and J. Brynolfsson, "The scaled reassigned spectrogram with perfect localization for estimation of Gaussian functions," *IEEE Signal Processing Letters*, vol. 22, no. 1, pp. 100–104, 2015.

[12] M. Sandsten, R. Anderson, I. Reinhold, and J. Brynolfsson, "The matched reassigned cross-spectrogram for phase estimation," in *Proceedings of the ICASSP*. Barcelona, Spain: IEEE, 2020, virtual.

[13] C. Kerrén, I. Bramão, R. Hellerstedt, and M. Johansson, "Strategic retrieval prevents memory interference: the temporal dynamics of retrieval-orientation," *Neuropsychologia*, 2021, 107776.

[14] B. He, L. Astolfi, P. A. Valdés-Sosa, D. Marinazzo, S. O. Palva, C.-G. Bénar, C. M. Michel, and T. Koenig, "Electrophysiological brain connectivity: Theory and implementation," *IEEE Trans. on Biomed. Eng.*, vol. 66, no. 7, 2019.

[15] R. G. Baraniuk, P. Flandrin, A. J. E. M. Janssen, and O. J. J. Michel, "Measuring time-frequency information content using Rényi entropies," *IEEE Trans. on Information Theory*, vol. 47, no. 4, pp. 1391–1409, May 2001.